Charge transport and ammonia sensing properties of flexible polypyrrole nanosheets grown at air-liquid interface

Elsevier Editorial System(tm) for Sensors & Actuators: B. Chemical
Manuscript Draft

Manuscript Number:

Title: Charge transport and ammonia sensing properties of flexible polypyrrole nanosheets grown at air-liquid interface

Article Type: Research Paper

Keywords: Polypyrrole, nanosheets, Mott's law, ammonia, gas sensors

Corresponding Author: Dr. Niranjan Suryakant Ramgir,

Corresponding Author's Institution: Bhabha Atomic Research Center

First Author: Purushottam Jha

Order of Authors: Purushottam Jha; Niranjan Suryakant Ramgir; Preetam K Sharma; Niyanta Datta; Kailasaganapathi S; Manmeet Kaur; Shankar P Koiry; Vibha Saxena; Anil K Debnath; Anil K Chauhan; Ajay Singh; Dinesh K Aswal; Shiv K Gupta

Abstract: Flexible polypyrrole nanosheets (thickness ~150 nm) grown at the air-liquid interface have been investigated for charge transport and NH3 sensing application. Polypyrrole nanosheets films were mechanically strong and exhibited a uniform and dense morphology. Temperature dependent charge transport measurements revealed that the PPy films obey Mott's 3-D variable range hopping mechanism. The mobility values calculated using temperature dependent current voltage characteristics indicated them to obey Arrhenius behavior. These films exhibited a reversible response towards NH3 at room temperature. The sensor exhibited a sensitivity of ~12% with a typical response and recovery times of 240 s and 50 min, respectively towards 50 ppm of NH3. Raman studies indicated that there is an increase in the antisymmetrical C-N stretching upon exposure to higher concentration of NH3 (500 ppm) and could be assigned to the interaction of NH3 with the carbon backbone of PPy film. Our results clearly emphasize that these flexible PPy films could be used to realize flexible sensors.

Suggested Reviewers: Shyam Aravamudhan
saravamu@ncat.edu

Vinayak Dravid
v-dravid@northwestern.edu

Ashok Mulchandani
adani@engr.ucr.edu

Pi-Guey Su
spg@faculty.pccu.edu.tw

Sudipta Seal
sseal@mail.ucf.edu

Charge transport and ammonia sensing properties of flexible polypyrrole nanosheets grown at air-liquid interface

Purushottam Jha, Niranjan S. Ramgir,* Preetam K. Sharma, N. Datta, S. Kailasaganapathi, M. Kaur, S. P. Koiry, V. Saxena, A. K. Chauhan, A. K. Debnath, Ajay Singh, D. K. Aswal,* S. K. Gupta

Technical Physics Division, Bhabha Atomic Research Centre, Mumbai 400 085

E-mail: niranjanpr@yahoo.com

Abstract

Flexible polypyrrole nanosheets (thickness ~150 nm) grown at the air-liquid interface have been investigated for charge transport and NH_3 sensing application. Polypyrrole nanosheets films were mechanically strong and exhibited a uniform and dense morphology. Temperature dependent charge transport measurements revealed that the PPy films obey Mott's 3-D variable range hopping mechanism. The mobility values calculated using temperature dependent current voltage characteristics indicated them to obey Arrhenius behavior. These films exhibited a reversible response towards NH_3 at room temperature. The sensor exhibited a sensitivity of ~12% with a typical response and recovery times of 240 s and 50 min, respectively towards 50 ppm of NH_3. Raman studies indicated that there is an increase in the antisymmetrical C-N stretching upon exposure to higher concentration of NH_3 (500 ppm) and could be assigned to the interaction of NH_3 with the carbon backbone of PPy film. Our results clearly emphasize that these flexible PPy films could be used to realize flexible sensors.

Keywords: Polypyrrole, nanosheets, Mott's law, ammonia, gas sensors

1. Introduction

Conducting polymers (CPs) like polyanilene, polythiophene and polypyrrole (PPy) have been investigated elaborately because of their high electrical conductivity, ease of preparation, high and uniform yield and environmentally benign [1]. Their unique π-conjugated electronic system plays a crucial role in achieving high conductivity with subgap states [2,3]. Of these, PPy is a conducting polymer of the rigid-rod polymer host family, all basically derivatives of polyacetylene. Importantly, it was the first polyacetylene-derivative that exhibited a high conductivity. Additionally, it exhibited properties like good environmental stability, low toxicity and also has been demonstrated to produce changes in its color, mass, work function or electrical conductivity [4,5]. Accordingly, it has been investigated elaborately for potential applications including artificial muscles, fuel cell membrane [6], electromagnetic irradiation shielding materials, photovoltaic cells, coating materials, corrosion inhibitors, and chemical and biosensors [7,8,9,10]. In particular, for chemical sensors the PPy in the form of nanoparticles, nanowires and thin films have demonstrated an enhanced sensing performance towards NH_3 gas [11,12,13,14].

Ammonia in particular, is a poisonous, colorless gas with a characteristic pungent smell and has a fairly low odor threshold of approximately 0.6–53 ppm. It has a short term explosive limit of 35 ppm. The presence of ammonium salts at 200–500 mg/kg of body weight results in lung oedema, nervous system dysfunction, acidosis, and kidney damage. The interaction of PPy with ammonia is found to be reversible at low concentrations and short exposure times, however longer exposures to higher concentrations produce irreversible effects [15]. PPy film undergoes a complex reversible redox reaction during ammonia detection. Besides, they possess advantages in comparison to metal-oxide gas sensors like capability to operate at room temperature, bulk penetration by analytes, and tunable selectivity/sensitivity. The free standing PPy films having good mechanical strength could also be effectively used for fabricating flexible sensors. The fabrication of electronic devices on flexible substrates is of technological importance. The applications of flexible sensors are complementary to that

of conventional sensors. For example, they can be used in handheld and portable consumer electronics [16], aero-space applications and civil engineering [17].

In the present work, the charge transport and NH_3 sensing properties of flexible PPy nanosheets synthesized by a novel route using j-aggregates of porphyrin derivatives as in-situ templates have been investigated [18]. The low temperature charge transport measurement indicated that the conductivity of PPy films obeys Mott's variable range hopping mechanism. The flexible PPy films sensor films could reversibly detect NH_3 at room temperature. The sensor film exhibited a sensitivity of ~12% with a typical response and recovery times of 240 s and 50 min, respectively towards 50 ppm of NH_3. A linear dependence of sensitivity on gas concentration upto 100 ppm (S%- 28) was observed.

2. Experimental Section

2.1. Methods and Materials

Pyrrole (98%) was procured from Aldrich and distilled over calcium hydride under reduced pressure prior to use. Anhydrous $FeCl_3$ (LR grade) was purchased from Thomas Baker. The organic solvents namely dichloromethane (DCM), chloroform were of analytical grade and Millipore water was used for solution preparation and washing. The 5-(4-hydroxyphenyl)-10,15,20-triphenylporphyrin (TPPOH) was synthesized using the procedure reported elsewhere [16].

2.2. Nanosheets growth

Two types of free standing PPy films were synthesized using interfacial polymerization at air-liquid interface. The growth process is elaborated below:

1. PPy using TPPOH template: Our one pot fabrication strategy for the growth of free standing PPy nanosheets involves the use of spontaneously formed TPPOH j-aggregate films at air/aqueous $FeCl_3$ interface as an in-situ template. Briefly, to a 80 ml of 0.1 M aqueous $FeCl_3$ solution in a beaker a 200 µL solution consisting of 1 mM TPPOH and 0.1 M pyrrole in DCM was slowly dropped using a micropipette. When a solution containing mixture of TPPOH and pyrrole in DCM is dropped, first TPPOH immediately forms a film at the air/liquid interface which is due to rapid

j-aggragation i.e., aggregation of monomeric units stacking into edge-to-edge configurations, of TPPOH. Now as the growth of PPy is a slower process compared to j-aggreagtion of TPPOH, these films grow as a sandwich layer between TPPOH and the liquid interface. J-aggregation and the template action of the TPPOH have already been confirmed using UV-vis and FTIR spectroscopic measurements as reported earlier [16]. Films formed at the air-aqueous interface were mechanically strong and lifted easily on microglass slides after 24 h and washed repeatedly (5 times) with millipore water and DCM to remove the traces of $FeCl_3$ and j-aggregate template.

2. PPy without the TPPOH template: Briefly, to a 80 ml of 0.1 M aqueous $FeCl_3$ solution in a beaker a 200 µL solution consisting of 0.01 M pyrrole in DCM was slowly dropped using a micropipette [16]. It requires more than 20 min for the free standing films to be formed at the air-liquid interface. The resulting films were highly porous in nature and most of them ruptured into small islands when attempted for transfer onto the microglass slides.

All the films were washed thoroughly using Millipore water and then used for further characterization and application.

2.3. Nanosheets characterization

Surface morphology of the as-grown films were investigated using scanning electron microscopy (SEM) TESCAN, Model TS 5130MM. Raman spectrum was collected using a microscopic confocal Raman spectrometer (HORIBA Jobin Yvon, Lab RAM HR) employing a 514 nm laser beam and using 100X objective at room temperature. Exposure to concentrations below 100 ppm did not exhibit a variation in the Raman signal. However, at higher exposure concentration of 500 ppm a change in signal is observed.

2.4. Low temperature conductivity measurements

For low temperature conductivity measurements two probe configuration was used. The charge transport measurements were carried out using in-plane electrode geometry. For this purpose, two planar gold electrodes of length 3 mm, width 2 mm with 12 µm electrode spacing were thermally deposited onto films using a metal mask and silver wires were attached to the gold pads with silver

paint. The IV measurements were carried out using Keithley 6487 picoammeter/voltage source and Labview based data acquisition system. The measurements at low temperatures (300-50K) were carried out using a closed cycle cryostat. All measurements were performed in dark to avoid the problem of photoconductivity. Conductivity measurements were carried out in a helium gas environment.

2.5.Gas sensing measurements

Gas sensing measurements were performed in a static environment method as reported elsewhere [19]. In brief, an interdigitated array (IDA) electrode of Au was first thermally deposited onto the sensor films. IDA represents the most suitable geometry to serve as a transducer in chemi-resistive gas sensors. A Pt wire heater was attached at the backside of the glass substrate to maintain and control the operating temperature of the sensor. The sensor films were mounted upside down in a leak tight stainless steel chamber having volume of 250 cm^3. Required concentration of a test gas in the chamber was attained by introducing a measured quantity of desired gas using a syringe. The response curves towards various test gases were measured by applying a fix bias of 0.1 V across the electrode and the time dependence of the current was recorded using PC based data acquisition system using Labview software. Once a steady state was achieved, recovery of sensors was recorded by exposing the sensors to air, which is achieved by opening the lid of the chamber. The sensitivity (S (%)) of the sensors was calculated from the response curves using the relation:

$$S\ (\%) = \frac{|I_g - I_a|}{I_a} \times 100\ \% \qquad \text{- (1)}$$

where, I_g and I_a are current values of the sensor films in test gas and fresh air, respectively. Response and recovery times were defined as the times needed for 90% of total change in resistance upon exposure to test gas and fresh air, respectively.

3. Results and Discussion

3.1. Morphological Characterization

Figure 1 shows the SEM images of the as grown films transferred onto the microglass slide substrates. PPy films grown without the TPPOH template (Figure 1 (a)) exhibited a porous morphology attributed

to the slow kinetics of the interfacial polymerization of PPy. The porous nature of the film is clearly evident from the high magnification image as shown in Figure 1 (b). Most of the films ruptured into small islands when attempted for transfer onto the substrates. This further implies that PPy films grown without the TPPOH template are not mechanically strong. Hence were not investigated in detail for further experiments. On the other hand, PPy films grown using TPPOH template are observed to maintain the similar i.e., j-aggregate morphology of the TPPOH template as shown in Figure 1 (b). Herein, the –N-H group of pyrrole rings forms hydrogen bonding with porphyrin core of the j-aggregates. This further provides the directionality for polymerization in the form of nanothreads. High magnification image (Figure 1 (d)) shows that the film is highly uniform with dense morphology and devoid of pores. These films were mechanically strong and do not rupture or break when attempted to transfer on substrates.

3.2. Low temperature conductivity measurements

The electronic properties of the conducting polymers are very much dependent on the structural aspects like the orientation, conformation, chain length, etc. The transport properties are also affected by the defects, disorders and presence of dopants ions. Polarons and bipolarons are localized states with finite mobility. PPy grown using the present strategy are very weakly doped (Cl^-) as is evident from the conductivity values and was also proven with the help of Uv-vis measurements [16,20]. A decision about the conduction mechanism is often comprehended based on the type of temperature dependence of the conductivity [21, 22]. The temperature dependence of d. c. electrical resistivity $\rho(T)$ of the PPy films grown using TPPOH template (Figure 2 (a)) revealed that the ρ increases with lowering temperature indicating a critical or insulating behavior of the films in the whole range of investigation. The temperature dependence of the reduced activation energy, described as:

$$W = -\,\mathrm{d}\ln[\rho(T)]/\mathrm{d}\ln T \qquad \text{- (2)}$$

is plotted in Figure 2 (b) [23]. Positive, zero and negative slopes of W vs T corresponds to the metallic, critical and insulating regimes, respectively. A negative slope for PPy film indicates that it is in the insulating regime.

For the sample in the insulating regime of the metal to insulator (M-I) transitions, the low temperature resistivity follows the exponential temperature dependence of variable range hopping conduction (VRH) (Figure 2 (c)) [20, 24]. In this model the resistivity of the disordered material is controlled by the hopping of charge carriers between local states near the Fermi level. When the Coulomb interaction between charge carriers is weak and can be neglected, then the Mott-VRH is applicable. In this case the temperature dependence of resistivity can be expressed as:

$$\rho(T) = \rho(0)\exp(T_0/T)^{\frac{1}{d+1}} \qquad \text{- (3)}$$

where, d is the dimensionality of the hopping process, T_0 is the characteristics Mott temperature and given as:

$$T_0 = \frac{18}{L_c^{\,3} N(E_F) k_B} \qquad \text{- (4)}$$

where, L_c is the localization length, $N(E_F)$ is the density of states at the Fermi energy. The typical value of $N(E_F)$ for moderately doped PPy is 2 x 10^{20} $eV^{-1}cm^{-3}$ [25]. The average hopping distance R_{hop} is related to the L_c and T_0 by relation:

$$R_{hop} = \frac{3}{8} L_C \left(\frac{T_0}{T}\right)^{\frac{1}{d+1}} \qquad \text{- (5)}$$

As seen in Figure 2 (c), for pure PPy films the temperature dependence of resistivity is best described by Motts 3D-VRH with T_0 = 2.34 x10^7 K. Using $N(E_F)$ as is 2 x 10^{18} $eV^{-1}cm^{-3}$, the estimated L_C and R_{hop} are 16.5 Å and 103 Å. The ratio $R_{hop}/L_c \sim 6$, indicates that in pure PPy films the carriers are strongly localized therefore making it close to the insulating behavior of M-I transition.

3.3. Current – voltage characteristics

Typical *J-V* characteristics recorded for PPy films, as shown in Figure 3, indicates that the variation of current depends on the applied bias. Based on the nature of *J* dependence on *V*, two distinct regions (marked as I to II in Figure 3) have been identified. The analyses of these regions are described below. As shown in Figure 3 (a), a transition from region I to region II takes place as a function of applied bias. In the region I, the slope of the linear fit to data is ~1, indicating an ohmic conduction. In molecular semiconductors, an ohmic conduction normally occurs if the thermally generated carriers exceed that of injected carriers through the electrode, and the *J* in this case is given by:

$$J = n_0 e \mu E \qquad \text{-(6)}$$

where, n_0 is the thermally generated hole concentration, e is electronic charge, μ is the hole mobility and d is the electrode separation [26]. However, the slope value in region II is ~2, indicating that the charge transport is via trap-free space-charge limited characteristics (SCLC). SCLC occurs if the injected carrier density is higher than the thermally generated carrier density and the *J* depends on applied bias using the relation:

$$J = \frac{9}{8} \varepsilon \mu \frac{V^2}{d^3} \qquad \text{- (7)}$$

where, ε is the permittivity of the film [23]. The typical reported value of ε for PPy films is 1.2×10^{-10} F/m [27]. Using data of Figure 3 (a), we have calculated the values of n_o and μ. The value of n_0 is determined from the crossover voltage (V_t), as shown in Figure 3 (a) and using the relationship: $V_t = 8 n_0 e d^2 / 9\varepsilon$. The estimated value of n_0 at 300K is 2.8×10^{20} m^{-3}, which is in agreement with the reported literature of organic semiconductor films [24]. The μ values at different temperatures were calculated from the slopes of J-V^2 plots. The μ value at 300K was found to be 5.34×10^{-5} m^2/V-s. The temperature dependence of μ is plotted in Figure 3 (b), which is found to obey the Arrhenius behavior i.e. $\ln \mu \sim 1/T$.

3.4. Gas sensing properties

Two types of PPy films namely grown with and without the TPPOH templates were investigated for their NH_3 sensing properties. Under similar concentrations of the starting solutions the thickness of the films was identical. PPy films grown without the TPPOH template suffered from the inherent drawback of poor intergrain connectivity. Hence, it was difficult to get a continuous and uniform film onto the substrates. Most of the films ruptured forming islands when attempted for transfer. However, one of the successful attempts resulted in a reasonable film transfer onto the microglass slides and accordingly was investigated along with the PPy films grown using TPPOH template. The response curves recorded for PPy films grown with and without the templates are shown in Figure 4. PPy films grown without the template exhibited a response towards NH_3 only at room temperature. A typical response and recovery times towards 50 ppm of NH_3 were 150 s and 24 min, respectively. Besides, a linear dependence of sensitivity on gas concentration upto 100 ppm (S%-23) was observed. These films did not exhibit any response at higher temperatures greater than RT.

On the other hand films grown using TPPOH templates were quite stable and exhibited an enhanced sensitivity towards NH_3. A typical response and recovery times towards 50 ppm of NH_3 were 240 s and 50 min, respectively. They also exhibited a linear dependence of sensitivity on gas concentration upto 100 ppm (S%- 28). Importantly, these films were mechanically strong and could easily be lifted onto the desired substrates. For comparison, we have also investigated the gas sensing properties of the PPy films but without the removal of template. As expected these films do not exhibited a response towards NH_3 due to the blocking action of TPPOH.

Figure 5 (a) shows the plot of sensitivity as a function of operating temperature for PPy films grown using TPPOH template towards 25 ppm of NH_3. The sensitivity of these films was found to decrease with increase in the operating temperature with maximum at room temperature. Long term stability measurements performed on these sensors as shown in figure 5 (b) indicated them to be

reasonably stable for over 25 days. The base line resistance changed from 72 to 242 kΩ while no significant variation in the sensitivity values was observed.

3.5. Sensing mechanism

Ammonia is a kind of electron donating gas and can donate to the initially oxidized PPy sensor film. Exposure to NH_3 has been demonstrated to result in both reversible as well as irreversible processes [28]. The interaction of PPy with ammonia is found to be reversible at low concentrations and short exposure times, whereas long exposure to higher concentrations produces irreversible effects [29]. As is evident from the response curves in the present case interaction of PPy with NH_3 takes place reversibly. The reversible changes have been assigned to compensation effects involving electron or proton transfer. For electron transfer compensation, NH_3 molecule compensates the electrical p-type charge created by the dopant anion molecule

$$PPy^+A^- + NH_3 \leftrightarrow PPy^0 \ — NH_3^+, A^- \qquad \text{- (8)}$$

Similarly, for proton transfer compensation, NH_3 attacks and removes the hydrogen atom attached to the heteroatom of the pyrrole ring via formation of ammonium ion NH_4^+. This eventually compensates the p-type charge induced by the dopant anion molecule. The overall effect is that the number of charge carriers on the polymer surface reduces making polymer more neutral causing conductivity to reduce.

Now this process is reversible when ammonium ion only binds very weakly to the negative anion facilitating the reverse reaction

$$PPy^+A^- + NH_3 \leftrightarrow [PPy(—H1^+)]^0 + NH_4^+A^- \qquad \text{- (9)}$$

Irreversible changes in polymers are mainly ascribed to the nucleophilic attack of NH_3 molecules on the carbon backbone. This attack introduces defects that shorten the conjugation length of the polymer chain. This leads to increase in disorder and decrease in conductivity as charge transport becomes more dominated by interchain hopping rather than charge transfer along the polymer chain.

3.6. Raman Investigations

In order to understand the nature of interaction between NH_3 and PPy, Raman investigations have been performed both in the presence and the absence of NH_3 gas. Accordingly, Figure 6 shows the Raman

spectra of the type I sample. In the absence of NH_3 the sample exhibited a peaks at 928, 985, 1045, 1249, 1332, 1405 and 1576 cm^{-1}. The peak at 928 is associated with the bipolaron, 1045 is assigned to the C-H in plane deformation. The small hump at 1249 cm^{-1} is assigned to the C-H in plane and the ring stretching, peak at 1332 to the ring-stretching mode, 1405 to the antisymmetrical C-N stretching and the peak at 1576 represents the C═C backbone stretching [30,31,32]. Now, upon exposure to small concentrations of NH_3 no significant variation in the Raman peak was observed. However, upon exposure to higher concentrations ~500 ppm a change in the Raman signals was observed. Although, the position of all the peaks remains same, the peaks at 928 and 1045 cm^{-1} decrease in intensity. This implies that there is a reduction in bipolaron density and decrease in the C-H in-plane deformation. Also, an increase in intensity of peaks at 1332, 1405 and 1576 cm^{-1} is observed and could be attributed to the increase in ring-streching mode, antisymmetrical C-N stretching and C═C backbone stretching. This further confirms that upon higher dose of exposure (500 ppm) NH_3 molecules attacks on the carbon backbone and could result in irreversible changes in PPy film.

Conclusions

Polypyrrole nanosheet films grown at the air-liquid interface have been investigated for charge transport and NH_3 sensing application. These films were mechanically strong and could easily be lifted onto the desired substrates. Charge transport measurements revealed that conductivity of the PPy films obeys Mott's 3-D variable range hopping mechanism. The mobility values calculated using temperature dependent current voltage characteristics indicated them to obey Arrhenius behavior. Additionally, these films exhibited a reversible response towards NH_3 at room temperature. A typical response and recovery times towards 50 ppm of NH_3 were 240 s and 50 min, respectively with sensitivity (S%) of ~12%. They also exhibited a linear dependence of sensitivity on gas concentration upto 100 ppm (S%- 28). Raman studies indicated that there is an increase in the antisymmetrical C-N stretching upon exposure to higher concentration of NH_3 (500 ppm) and could be assigned to the interaction of NH_3 with the carbon backbone of PPy film. Thus, our results clearly indicate that the PPy films could be looked upon as a potential candidate for realizing flexible sensors.

Acknowledgments

This work is partly supported by “DAE-SRC Outstanding Research Investigator Award” (2008/21/05-BRNS) and “Prospective Research Funds” (2008/38/02-BRNS) granted to D.K.A.

References

[1] F. Faverolle, A. J. Attias, B. Bloch, P. Audebert, C. P. Andrieux, Highly conducting and strongly adhering polypyrrole coating layers deposited on glass substrates by a chemical process, Chem. Mater. 10 (1998) 740-752.

[2] X. Zhang, J. Zhang, W. Song, Z. Liu, Controllable Synthesis of conducting polypyrrole nanostructures, J. Phys. Chem. B 110 (2005) 1158–1165.

[3] S. Pirsa, N. Alizadeh, Design and fabrication of gas sensor based on nanostructure conductive polypyrrole for determination of volatile organic solvents, Sens. Actuators B 147 (2010) 461–466.

[4] J. W. Gardner, P. N. Bartlett, A brief history of electronic noses, Sens. Actuators B 18/19 (1994) 211–220.

[5] C. C. Bof Bufon, J. Vollmer, T. Heinzel, P. Espindola, H. John, J. Heinze, Relationship between chain length, disorder, and resistivity in polypyrrole films, J. Phys. Chem. B 109 (2005) 19191-19199.

[6] H. S. Park, Y. J. Kim, W. H. Hong, H. K. Lee, Physical and electrochemical properties of Nafion/polypyrrole composite membrane for DMFC, J. Membrane Sci. 272 (2006) 28-36.

[7] A. Joshi, S.A. Gangal, S.K. Gupta, Ammonia sensing properties of polypyrrole thin films at room temperature, Sens. Actuators B 156 (2011) 938– 942.

[8] S. C. Hernandez, D. Chaudhuri, W. Chen, N. V. Myung, A. Mulchandani, Single polypyrrole nanowire ammonia gas sensor, Electroanalysis 19 (2007) 2125-2130.

[9] X. Ma, X. Zhang, Y. Li, H. Yu, G. Li, M. Wang, H. Chen, Gas sensing behavior of nano-structured polypyrrole prepared by “carbon nanotubes seeding” approach, J. Nanopart. Res. 10 (2008) 289.

[10] S. Cosnier, Biosensors based on immobilization of biomolecules by electrogenerated polymer films; New perspectives, Appl. Biochem. Biotechnol. 89 (2000) 127-138.

[11] L. Zhang, F. Meng, Y. Chen, J. Liu, Y. Sun, T. Luo, M. Li, J. Liu, A novel ammonia sensor based on high density, small diameter polypyrrole nanowire arrays, Sens. Actuators B 142 (2009) 204–209.

[12] N. Chartuprayoon, C. M. Hangarter, Y. Rheem, H. Jung, N. V. Myung, Wafer-scale fabrication of single polypyrrole nanoribbon-based ammonia sensor, J. Phys. Chem. C 114 (2010) 11103–11108.

[13] O. S. Kwon, J.-Y. Hong, S. J. Park, Y. Jang, J. Jang, Resistive gas sensors based on precisely size-controlled polypyrrole nanoparticles: effects of particle size and deposition method, J. Phys. Chem. C 114 (2010) 18874–18879.

[14] S. Carquigny, J.-B. Sanchez, F. Berger, B. Lakard, F. Lallemand, Ammonia gas sensor based on electrosynthesized polypyrrole films, Talanta 78 (2009) 199–206.

[15] Q. Ameer, S. B. Adeloju, Polypyrrole-based electronic noses for environmental and industrial analysis, Sens. Actuators B 106 (2005) 541–552.

[16] M. C. McAlpine, H. Ahmad, D. Wang, J. R. Heath, Highly ordered nanowire arrays on plastic substrates for ultrasensitive flexible chemical sensors, Nature Mater. 6 (2007) 379 - 384.

[17] Y. Sun, H. Hau Wang, High-performance, flexible hydrogen sensors that use carbon nanotubes decorated with palladium nanoparticles, Adv. Mater. 19 (2007) 2818–2823.

[18] P. Jha, S. P. Koiry, V. Saxena, P. Veerender, A. K. Chauhan, D. K. Aswal, S. K. Gupta, Growth of free-standing polypyrrole nanosheets at air/liquid interface using j-aggregate of porphyrin derivative as in-situ template, Macromolecules 44 (2011) 4583-4585.

[19] N. Datta, N. S. Ramgir, M. Kaur, S. Kailasaganapathi, A.K. Debnath, D.K. Aswal, S.K. Gupta, Selective H_2S sensing characteristics of hydrothermally grown ZnO-nanowires network tailored by ultrathin CuO layers, Sens. Actuators B 166– 167 (2012) 394– 401.

[20] D. Y. Kim, J. Y. Lee, D. K. Moon, C. Y. Kim, Stability of reduced polypyrrole, Synth. Met. 69 (1995) 471-474.

[21] P. Ohlckers, P. Pipinys, Phonon-assisted tunneling in charge transport of polypyrrole thin films and nanofibers, J. Appl. Phys. 109 (2011) 083713.

[22] K. Sato, M. Yamaura, T. Hagiwara, K. Murata, M. Tokumoto, Study on the electrical conduction mechanism of polypyrrole films, Synth. Met. 40 (1991) 35-48.

[23] T. A. Skotheim, R. L. Elsenbaumer, J. R. Reynolds, Eds., Handbook of conducting polymers, 2nd ed., Marcel Dekker Inc. Newyork (1998).

[24] N. F. Mott, Metal–insulator transition 2nd edition, Talor-Francis London (1990) and references therein.

[25] M. Ghosh, A. Barman, A. Das, A. K. Meikap, S. K. De, S. Chatterjee, Electrical transport in paratoluene sulfonate doped polypyrrole films at low temperature, J. Appl. Phys. 83 (1998) 4230-4235.

[26] S. Samanta, D. K. Aswal, A. Singh, A. K. Debnath, M. Senthil Kumar, Y. Hayakawa, S. K. Gupta, J. V. Yakhmi, Bias and temperature dependent charge transport in high mobility cobalt-phthalocyanine thin films, Appl. Phys. Lett. 96 (2010) 013305-3.

[27] C. C. Bof Bufon, T. Heinzel, Transport properties of chemically synthesized polypyrrole thin films, Phys. Rev. B 76 (2007) 245206-6.

[28] N. T. Kemp, A. B. Kaiser, H. J. Trodahl, B. Chapman, R. G. Buckley, A. C. Partridge, P. J. S. Foot, Effect of ammonia on the temperature-dependent conductivity and thermopower of polypyrrole, J. Poly. Sci. B 44 (2006) 1331-1338.

[29] Q. Ameer, S. B. Adeloju, Polypyrrole-based electronic noses for environmental and industrial analysis, Sens. Actuators B 106 (2005) 541–552.

[30] M. Li, J. Yuan, G. Shi, Electrochemical fabrication of nanoporous polypyrrole thin films, Thin Solid Films 516 (2008) 3836–3840.

[31] J. Arjomandi, A. A. Shah, S. Bilal, H. V. Hoang, R. Holze, In situ Raman and UV–vis spectroscopic studies of polypyrrole and poly(pyrrole-2,6-dimethyl-β-cyclodextrin), Spectrochim. Acta A 78 (2011) 1–6.

[32] H. Nguyen Thi Le, M.C. Bernard, B. Garcia-Renaud, C. Deslouis, Raman spectroscopy analysis of polypyrrole films as protective coatings on iron, Synth. Met. 140 (2004) 287–293.

Figure captions

Figure 1. SEM images of (a) PPy film grown without TPPOH template, and (b) PPy film grown using TPPOH template with an inset showing the corresponding magnified images.

Figure 2. (a) The temperature dependence of d. c. electrical resistivity $\rho(T)$ of the PPy film grown using TPPOH template recorded with electrode separation of 12 μm, (b) the temperature dependence of the reduced activation energy and (c) exponential temperature dependence of variable range hopping.

Figure 3. (a) Typical J-V characteristics as a function of temperature and (b) the temperature dependence of μ.

Figure 4. Response curve behavior of (a) PPy film grown without TPPOH template, (b) PPy film grown using TPPOH template and (c) linear dependence of sensitivity of both the films as a function of gas concentration.

Figure 5. (a) Sensitivity as a function of operating temperature for Type I sensor towards 25 ppm of NH_3 and (b) Long term stability measurements for Type I sensors towards 25 ppm of NH_3.

Figure 6. Raman spectra of PPy films grown using TPPOH templates with and without the exposure to 500 ppm of NH_3.

Figure 1.

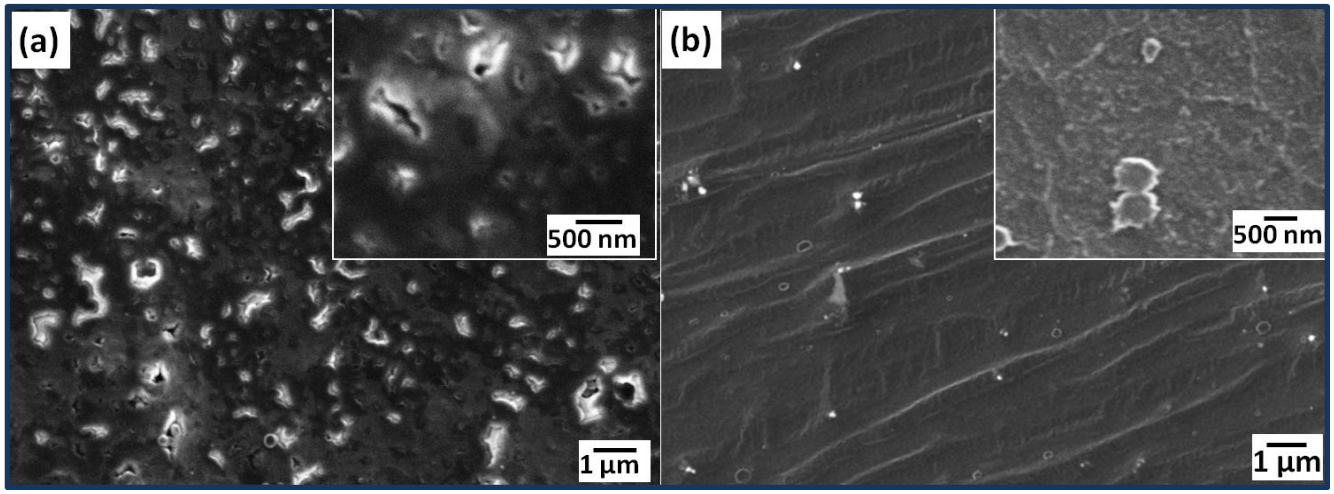

Figure 2.

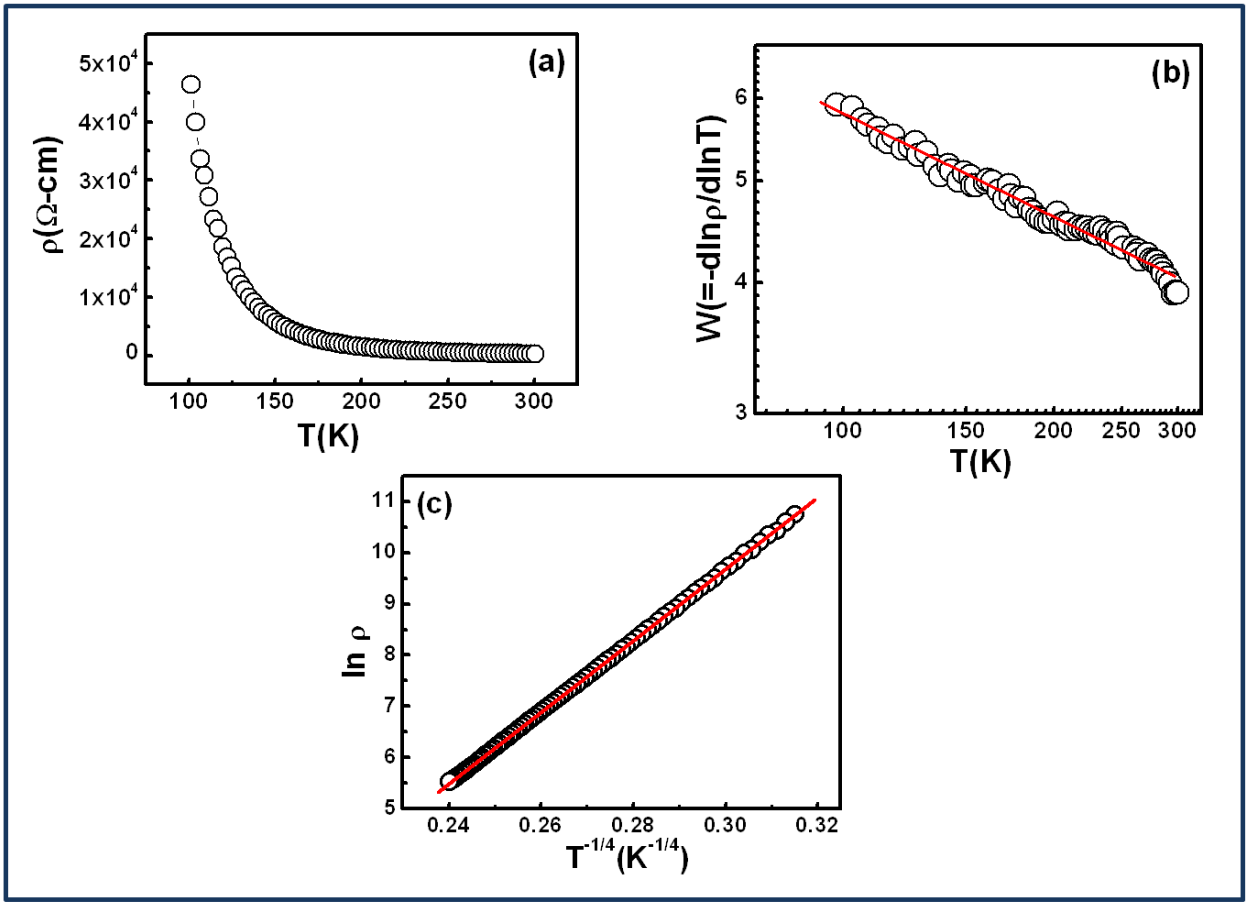
(a)
ρ(Ω-cm)
5x10^4
4x10^4
3x10^4
2x10^4
1x10^4
0
100
150
200
250
300
T(K)
(b)
W(=-dlnρ/dlnT)
6
5
4
3
100
150
200
250
300
T(K)
(c)
ln ρ
11
10
9
8
7
6
5
0.24
0.26
0.28
0.30
0.32
T^-1/4(K^-1/4)

Figure 3.

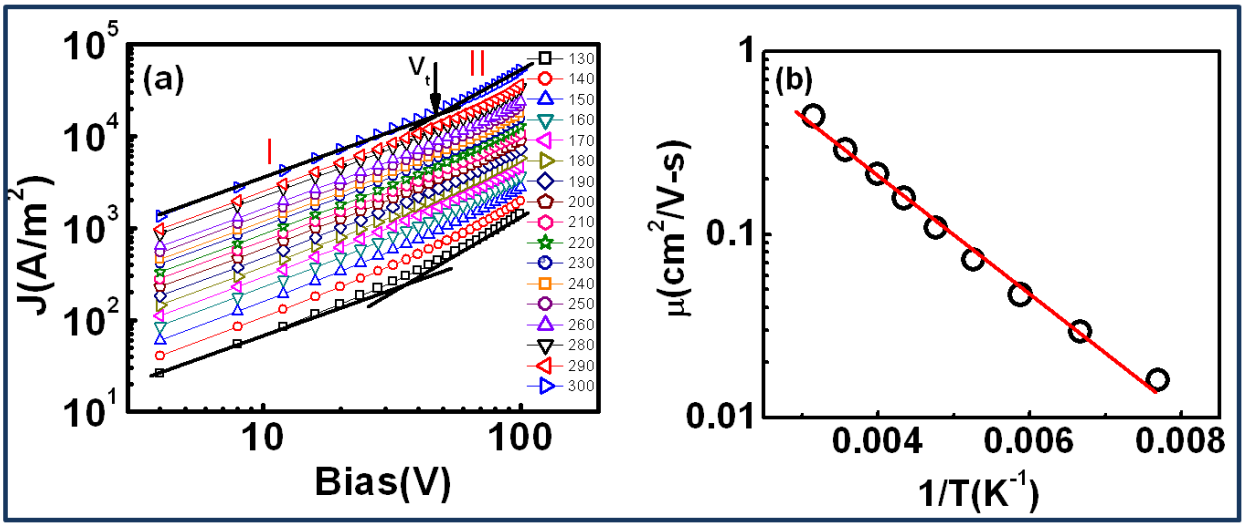
(a)
V_t
I
II
10^5
10^4
10^3
10^2
10^1
J(A/m^2)
10
100
Bias(V)
130
140
150
160
170
180
190
200
210
220
230
240
250
260
280
290
300
(b)
1
0.1
0.01
μ(cm^2/V-s)
0.004
0.006
0.008
1/T(K^{-1})

Figure 4.

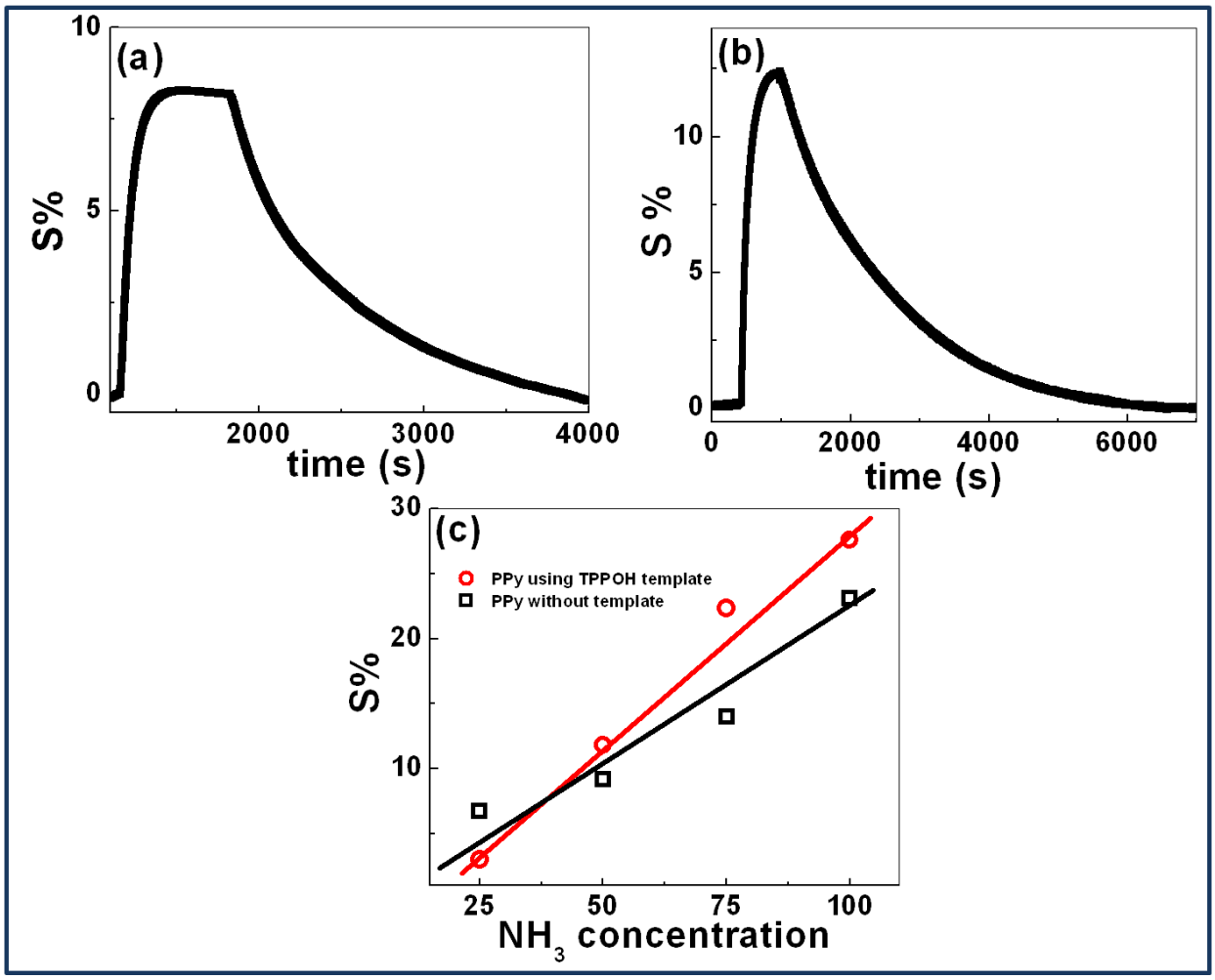
(a)
S%
time (s)
(b)
S %
time (s)
(c)
PPy using TPPOH template
PPy without template
S%
NH3 concentration

Figure 5.

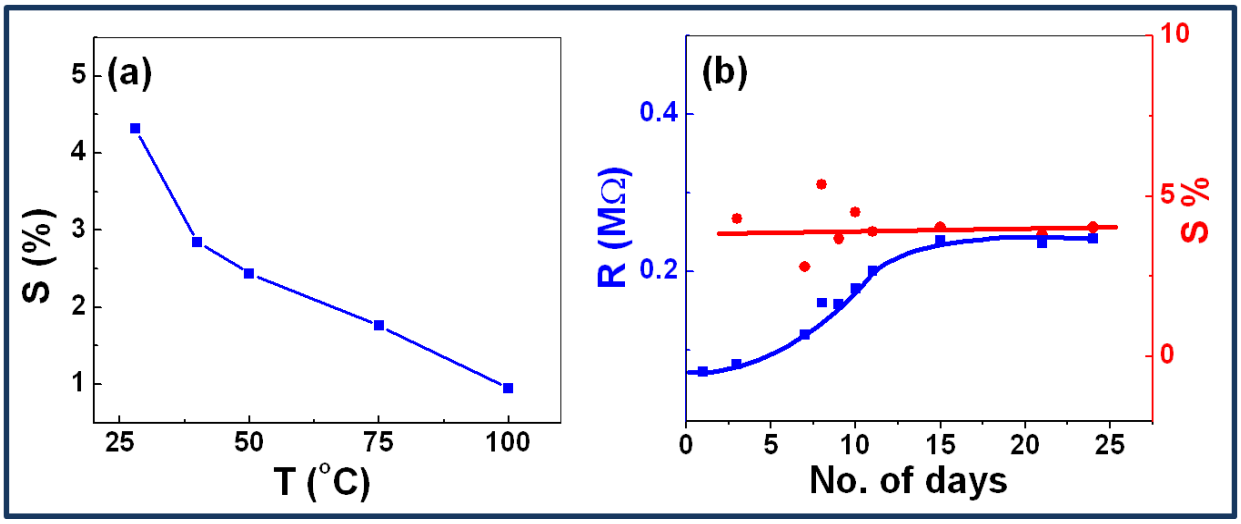

Figure 6.

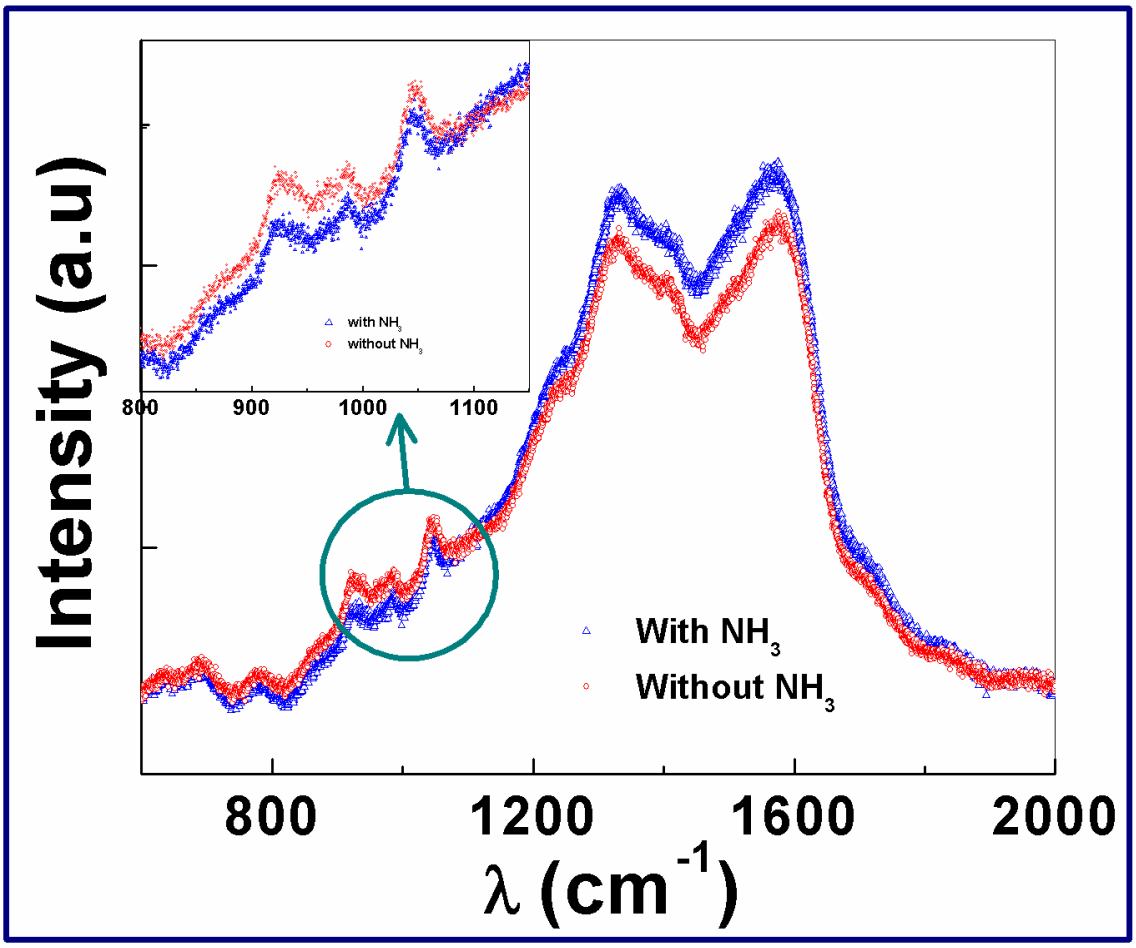
Intensity (a.u)
with NH3
without NH3
800
900
1000
1100
With NH3
Without NH3
800
1200
1600
2000
λ (cm-1)

Author's Biographies

Mr. Purushottam Jha joined BARC in 2008 as scientific officer after receiving M.Sc. (chemistry) from Banaras Hindu University, Varanasi. He has synthesized porphyrin derivatives and organic-inorganic nanocomposites for applications in molecular memories, gas sensors and field emission. He is currently pursuing his Ph.D. on conducting polymer based FET and gas sensors.

Dr. Niranjan Ramgir completed his PhD (Physics) in 2006 from National Chemical Laboratory, Pune, India. After completing his Humboldt fellowship at Nanotechnology Group, University of Freiburg, Germany, he joined BARC as Scientific Officer. His current research work is focused on applications of organic and inorganic semiconducting materials like polypyrrole, ZnO, WO_3, CuO and SnO_2 based thin films and nanostructures for sensing, e-nose and photovoltaic applications.

Mr. Preetam Kumar Sharma is presently working as a project trainee, at Technical Physics Division, BARC. He is pursuing his masters in nanotechnology at Centre for Converging Technologies, University of Rajasthan, Jaipur. His research interest includes study of growth and applications of organic and inorganic nanostructures for gas sensing and e-nose applications.

Ms. Niyanta Datta has completed her B.Sc. (Hons) in Physics from Delhi University and M.Sc in Physics from IIT Roorkee in 2008. She joined Bhabha Atomic Research Center through in 2008 through 52^{nd} batch of training school. Currently she is working as a scientific officer-C and her interests include study of charge transport and gas sensing properties of various nanostructures.

Mrs. S. Kailasaganapathi completed her B.Sc., in Physics from Manonmanium Sundaranar University, Tirunelveli, Tamilnadu, India in 2003. She joined Bhabha Atomic Research Center in 2006 as a Scientific Assistant. Her research work involves development of gas sensors based on metal-oxides.

Dr Manmeet Kaur received her PhD from Devi Ahilya Vishwavidyalaya, Indore in 1998. Her thesis work involved effect of heavy ion irradiation on high temperature superconductors. She joined Bhabha Atomic Research Center, Mumbai in 1999 as research associate. Her present interests include development of metal oxide thin films and nano-materials for sensing toxic gases.

Dr. S.P. Koiry joined BARC in 2004 as Scientific Officer after obtaining his M.Sc. (chemistry) from Assam University, Silchar. He submitted his PhD (HBNI, Mumbai) on studies for the development of molecular electronic devices in 2010. He is currently working on monolayer/multilayers of electrographted silane molecules, porphyrin derivatives and, organic dyes and self-assembled monolayers for various device applications.

Dr. Vibha Saxena joined BARC in 2004 as scientific officer. She received her Ph.D. (Physics) from Mumbai University in 2000. Over the years she worked on conducting polymer based light-emitting diodes, electrochemical transistors and biosensors. Her present interests are organic field-effect transistors, gas sensors and solar cells.

Dr. A.K. Debnath is presently working as Scientific Officer (F) at Technical Physics Division of BARC. He has extensively worked on oxide materials based gas sensor, particularly for H_2S detection. His current research interest is to understand the charge transport and gas sensing properties of ultra thin films of organic semiconductor grown using MBE.

Dr. Anil K. Chauhan joined BARC in 1992 through 36^{nd} Batch of Training School and is presently working as a Scientific Officer at Technical Physics Division of BARC. His research interest includes organic solar cells and electronics.

Dr. Ajay Singh joined BARC in 1999 through 42nd Batch of Training School after completing M.Sc. (Physics) from Garhwal University. He completed his Ph.D. from Mumbai University in 2004. Presently he is working on charge transport studies of metal phthalocyanine thin films and development of thermoelectric devices. He is a recipient of Humboldt Post-doctoral fellowship (2005–2007), DAE Young Scientist Award for excellence in the Science and Technology – 2007, National Academy of Sciences India (NASI) Young Scientist Platinum Jubilee Award – 2010 in Physical Science.

Dr. D. K. Aswal joined Bhabha Atomic Research Center in 1986 through 30th Batch of Training School after completing M.Sc. (Physics) from Garhwal University and is presently Head of Thin Films Devices Section. His area of scientific interest is condensed matter physics, specializing in device-oriented research leading to hybrid molecule-on-Si nanoelectronics, thermoelectric devices, and gas sensors. He is a recipient of several international fellowships including, JSPS fellowship, Japan (1997-99), IFCPAR fellowship, France (2004-05), BMBF fellowship, Germany (2006) and CEA fellowship, France (2008). He is recipient of several awards, including "MRSI Medal 2010", "Homi Bhabha Science and Technology Award -2007", "DAE-SRC Outstanding Research Investigator Award-2008", and "Paraj: Excellence in Science Award, 2000".

Dr. S. K. Gupta joined Bhabha Atomic Research Center in 1975 and is presently Head of Technical Physics Division. Over the years, he has worked on space quality silicon solar cells, high temperature superconductor thin films and single crystals, gas sensors and thermoelectric materials. He has carried out extensive studies on vortex dynamics in superconductors. He is a member of the National Academy of Sciences, India.